PAPER

Check for updates

From additive analysis to process monitoring: characterization of polypropylene solvent-based recycling from plastic feedstocks representative of sorting centres

Sofiane Ferchichi, [ID] abc Nida Sheibat-Othman, [ID] *b Maud Rey-Bayle [ID] a and Vincent Monteil [ID] *c

In between mechanical and chemical recycling, the recycling by dissolution/precipitation method has emerged as an economically and sustainably viable solution. This work addresses the challenges of this recycling method, particularly those related to the complex and diverse composition representative of polymers feedstocks from sorting centers, from an analytical perspective. We used various analytical tools, ranging from off-line chromatography coupled with high resolution mass spectrometry (LC-HRMS) to *in situ* spectroscopy, as well as thermal and fractionation analysis, to deeply characterize the plastic feedstocks at different stages of the recycling process. LC-HRMS and thermal gradient interaction chromatography (TGIC) provide valuable insights into the composition of market-available plastics feedstocks and the efficiency of sorting center operations. *In situ* NIR and Raman spectroscopy allowed real-time monitoring of the dissolution step to ensure complete dissolution, as well as the precipitation step to ensure effective polymer/additive separation. *Ex situ* attenuated total reflectance infrared spectroscopy (ATR-IR), differential scanning calorimetry (DSC), high temperature size exclusion chromatography (HT-SEC), and LC-HRMS confirmed that the recovered polymer after recycling maintained its properties while removing a fraction of additives. Also, we show that substitution of fossil-based solvents like xylene and decalin is possible by more responsible solvents like amyl acetate or cyclohexanone with comparable dissolution and additives removal performances.

Sustainability spotlight

The work presents a robust analytical workflow to monitor and optimize solvent-based recycling of polypropylene. The proposed strategy addresses the challenges related to the recycling of complex plastic feedstocks from sorting centers and demonstrate that greener solvents can effectively replace fossil-based ones with similar dissolution or additive removal efficiency. A key achievement of this work is the integration of real-time process control with pre- and post-recycling characterization, enabling a comprehensive assessment of recycling quality; the developed analytical workflow shows that up to 60% to 80% of additives can be removed while preserving polymer properties across various solvent and operating condition combinations. The work clearly aligns with the UN's Sustainable Development Goal 9 "Build resilient infrastructure, promote inclusive and sustainable industrialization and foster innovation".

1. Introduction

Sustainable management of plastic waste has become a global priority, so the development of plastic recycling processes has become an actual challenge. Recycling reduces reliance on fossil resources, thereby contributing to environmental preservation by transforming plastic waste into reusable raw materials. Also, these processes address issues related to improper

plastic disposal. Among recycling methods, mechanical recycling, which consists of melting and reshaping the plastic, has proven to be efficient to a certain extent. However, its repeated cycles often lead to polymer degradation, reduced molecular weight, and inferior material properties, which limits its applicability for high-performance products. Chemical recycling introduces a new dimension by breaking down plastics into their molecular components. This approach holds importance as it allows for the regeneration of high-quality raw materials, overcoming some of the limitations of mechanical recycling, especially with complex or contaminated plastic waste. Several chemical recycling routes are currently under development, including pyrolysis, gasification, and depolymerization, each offering distinct advantages depending on the

a IFP Energies Nouvelles, Rond-Point de l'échangeur de Solaize, 69360 Solaize, France

b Universite Claude Bernard Lyon 1, LAGEPP, UMR 5007 CNRS, 69622 Villeurbanne, France. E-mail: nida.othman@univ-lyon1.fr

c Universite Claude Bernard Lyon 1, CP2M, UMR 5128, CNRS, 69616 Villeurbanne, France. E-mail: vincent.monteil@univ-lyon1.fr

polymer type and waste stream. Solvent-based recycling emerges as a particularly impactful methodology.[1] This approach involves dissolving plastic waste in a selected solvent, leading to the separation of polymers from contaminants and additives. As an example, xylene as solvent and iso-propanol as antisolvent were used for the recovery of low-density polyethylene (LDPE) from plastic feedstocks representative of sorting centres.[2] Other recent works propose the use of green, bio-based solvents, for polyolefins dissolution like *p*-cymene, D-limonene or α-pinene.[3,4] In some cases, the additives can be recycled. For instance, supercritical carbon dioxide (CO_2) was used as antisolvent for extracting flame retardant additives.[5] This method not only addresses the limitations of mechanical recycling, but also provides a pathway to efficiently manage diverse plastic streams, promoting circular economy practices. Note that a specific technique exists for recycling multilayer plastic packaging materials, known as the Solvent Target Recovery and Precipitation (STRAP) process,[6–9] which supports that solvent-based recycling is a sustainable option in terms of life cycle assessment.

Meanwhile, online process monitoring holds significant importance across various industrial sectors, playing a crucial role in ensuring safety, reliability, and operational efficiency. More particularly, online process monitoring is essential for securing the facilities and operators by identifying any deviations from pre-established standards to prevent potential accidents and enable real-time corrective measures. Hence, process monitoring ensures operational fidelity, thus resulting in more a consistent production and higher-quality products. It can also be used for real-time optimization and finetuning of operating conditions, to enhance the process productivity and efficiency. Spectroscopic techniques, being non-invasive and providing fast and reliable data, represent excellent candidates for process monitoring.[10] For instance, near Infrared spectroscopy (NIR) is a common and versatile tool for process monitoring. It has increasingly been used for online monitoring of polymerization system due to sensitivity to monomer and polymer bands.[11–13] It can therefore be used for the understanding of the dissolution/reprecipitation process. Raman spectroscopy is also used for process monitoring[14] and known to be complementary to NIR, so they can be used together for a better description.[15]

At this date, the solvent-based recycling studies perform characterizations of the samples offline, before its recycling and of the purified polymer after its recycling, but none monitor in real-time the recycling process. However, real-time monitoring of solvent-based recycling processes appears as evident to accelerate the development of the recycling methods.

We have recently developed a process to treat plastic feed containing polymers with a dissolution step,[16] and a generalised method to monitor polypropylene dissolution across different solvents.[17,18] In this work, we propose to employ the developed monitoring methods, besides other characterizations, to enhance comprehension of plastic feedstocks representative of sorting centres during recycling processes, with a focus on mostly polypropylene (PP) feedstocks.

In the present work, we propose first to use classical characterization techniques to determine the chemical, structural and thermal properties of the plastic feedstocks representative of sorting centres. We also detect the additives present in the charge through a non-target screening process, by using liquid chromatography-high resolution mass spectrometry (LC-HRMS). This technique is usually used to detect and identify unknown compounds in a sample without prior knowledge. It is commonly used for the detection and identification of additives in food-contact plastic packages for instance[19,20] in order to identify substances of potential concern like, bioaccumulative or toxic.[21,22] This approach enables to detect and characterize a wide array of chemical substances, including those not previously reported or anticipated. Here, we use it to detect additives in PP feedstocks. The main objective is to perform the analysis before and after dissolution and precipitation to determine the quality of the recycling steps, thereby providing a thorough understanding of the additive's behaviour and efficient extraction during the recycling process.

The second objective is to apply the previously developed *in situ* monitoring methodologies based on commercial polypropylene, to monitor polypropylene feedstocks representative of sorting centres dissolution and precipitation. Two different *in situ* spectral methods have been tested, namely near infrared and Raman spectroscopy. Initial chemometric models were built in several solvents using commercial polypropylene. These models have been combined using orthogonalization and applied to monitor the complete polypropylene recycling process.

2. Experimental section

2.1. Solvents

Acetonitrile (ACN), methanol (MeOH) and formic acid (HCOOH) were all Optima™ LC/MS Grade purchased from Fischer Scientific (France). Deionized water was obtained from a Milli-Q water purifier system (Millipore SAS, France). The reagent grades solvents xylene, *n*-decane, decahydronaphthalene (decalin), and amyl acetate were purchased from Sigma-Aldrich (France) and were used without further purification.

2.2. Solvent selection

The selection of the solvents was based on their solubility parameter similarity (compatibility) to polypropylene.[17,23] In the context of developing a comprehensive methodology for the dissolution-based recycling process of polymers, we have selected a range of solvents that, while not the most environmentally friendly, serve the purpose of establishing a robust and versatile process. By thoroughly understanding and optimizing this methodology, we can subsequently transpose and adapt these techniques to use greener, more sustainable solvent systems. This approach ensures that the initial development is rigorous and effective.

2.3. Polymers

Plastic feedstocks representatives of sorting centres, mainly PP-based, "flake form" were obtained.

The available plastic feedstocks samples are denominated wPP1, wPP2 and wPP3, all mainly composed of PP. Note that the wPP2 and wPP3 come from the same plastic charge stream except that wPP2 is recompounded.

The plastic feedstocks samples have been reshaped by cryogenic grinding in some experiments to study the shape effect. The granulometry measurement of the samples after griding is provided in Fig. S1 and Table S1.

2.4. Instruments

2.4.1. Raman spectroscopy. A Kaiser Optical Systems RXN2 Raman spectrometer equipped with a 785 nm laser of 400 mW power was used with an immersion probe of 12 mm in diameter. The acquisition conditions were as follow: 5 seconds of integration time, and 10 scans are averaged to give 1 spectrum each minute. The wavelength region ranges from 100 cm^{-1} to 3425 cm^{-1}.

2.4.2. NIR spectroscopy. *In situ* NIR analysis was performed using a Hellma–Falcata NEW XP6 immersion reflectance probe (Hellma GmbH & Co) 124 of 6 mm diameter with an optical path fixed at 5 mm. A spectrometer NIRS MATRIX F-II (Bruker) recording wavelengths within the 870–2500 nm spectral range with a resolution of 0.5 nm was used to acquire the calibration and validation sets. Each final spectrum obtained was the average of 20 scans, leading to 1 spectrum each minute. The software used with the spectrometer was OPUS (Bruker).

2.4.3. ATR-IR spectroscopy. Offline IR spectra (4000 to 400 cm^{-1}) were collected with a Nicolet™ iS50 FTIR spectrometer equipped with a diamond attenuated total reflection (ATR) unit. Each IR spectrum corresponds to an accumulation of 32 scans with a resolution of 4 cm.[1]

2.4.4. Cryogenic grinding of plastic samples. The "flakes" of each polymer type were separately transformed into a powder form by cryogenic grinding using a CryoMill (Retsch, Haan, Germany). Each jar is filled with 1 zirconium oxide grinding ball of 25 mm diameter and 6 g PP – "flakes" form. The closed jar is pre-cooled to a temperature of – 100 °C using liquid nitrogen circulation and kept at this temperature for 20 min. Grinding is performed in 9 cycles of 1 min each, at 25 Hz, interrupted by 30 s intermediate maintained cooling phases at 5 Hz. Grinding has been repeated to ensure a representative cumulative sample. Polyolefins are not subject to radical changes during cryogenic grinding,[24] nevertheless we ensured that the polymer properties remained unchanged (molar mass, branching, crystallinity, *etc.*) and only the form changes.

2.4.5. Particle size measurements. A Malvern Mastersizer 3000 with Aero S disperser (Malvern Instruments Limited, Worcestershire, UK) was used to measure the particle size in dry mode. Agglomerates were placed onto the hopper tray with a 4-mm hopper gap. A standard venturi disperser was used with a feed rate of 25%, using compressed air. Three replicates were run for each sample. Mie theory was used as the optical model with a material refractive index of 1.490 (corresponding to polypropylene).

2.4.6. Accelerated solvent extraction. Pre-weighed samples (1.2 g) of grinded PP were put to the extraction cell. The extraction solution was a 66 : 34 mixture of toluene/methanol. 3

Extraction cycles were performed for each sample. Two microliters of each of these solutions was injected into LC-HRMS for analysis. Prior to each analysis, a blank run with toluene/methanol was performed to ensure the baseline was free from any residues or contaminants, thereby ensuring the precision and reproducibility of the measurements.

2.4.7. Liquid chromatography high resolution mass spectrometry (LC-HRMS). Liquid chromatography was performed using an Agilent 1290 UHPLC system (Agilent, USA) composed of a binary pump, an autosampler, a column manager and a photodiode array UV detector. The chromatographic system was coupled to a trapped ion mobility quadrupole-time-of-flight mass spectrometer (first generation timsTOF, Bruker Daltonics, Germany) through an electrospray ionization (ESI) interface (Apollo II, Bruker Daltonics, Germany). The calibration of the time-of-flight (TOF) analyzer was performed with a sodium formiate standard solution prior to analysis. A calibration segment was also placed before the column's dead time, allowing for precise external calibration with standard deviation around 0.2 ppm. The high-resolution mass spectrometer consists of (i) a TIMS cell, (ii) a quadrupole, (iii) a collision cell and (iv) a TOF analyzer. The device control was performed through HyStar v3.2 using the Agilent Instrument Control Framework (ICF) plug-in and Otofcontrol software respectively (Bruker Daltonics, Germany).

2.4.8. Chromatographic tuning parameters. The autosampler's temperature was set to 10 °C and the injection volume to 1 μL. A Kinetex Biphenyl separation column was used (150 × 3 mm, particle size 2.6 μm, Phenomenex, France) at 40 °C. The mobile phase solvents were: (phase A) H_2O milliQ (v/v) + 0.05% (v/v) formic acid in water and (phase B) a 50/50 (v/v) mixture ACN/MeOH + 0.05% (v/v) formic acid. The flow rate was 600 μL min^{-1}, and the following linear gradient was applied: 0.0–1.0 min: 25% (phase B); 1.0–35.0 min: from 25% to 100% (phase B); 35.0 to 42.0 min: 100% (phase B), 42.0–42.1 min: 100% to 25% (phase B); 42.1–52.0 min: 25% (phase B).

2.4.9. Mass spectrometry tuning parameters. For the high-resolution mass spectrometry (HRMS) experiments in positive and negative ionization mode, the tuning parameters are the scan range: 50–1500 *m/z*, spectra rate: 3 Hz, end plate offset: 500 V, capillary voltage: 4000 V, nebulizer pressure: 55 psi, dry gas flow rate: 9.0 L min^{-1} and dry gas temperature: 200 °C. The funnels transfer parameters were optimized to provide a maximum analytical sensitivity. The TIMS cell was not used as we did not expect further separation from it.

2.4.10. LC-HRMS data processing. Data processing was performed using MetaboScape® 2024b software (Bruker Daltonics, Germany) using the T-ReX 3D algorithm. The LC-HRMS data of the plastic feedstocks, the respective effluents obtained after dissolution/precipitation, and 3 blanks (control) were used for processing. The following parameters were used for feature selection: the minimum peak length was set to 6 spectra and intensity thresholds of 10 000 counts and 5000 counts were applied for feature detection in positive and negative modes, respectively. A recursive feature extraction with a minimum peak length of 4 was also applied. The 0.0–0.5 min interval was used for formate adduct internal calibration. The mass-to-

charge ratio and retention time (RT) range for feature detection were set to 50–1500 and 0.5–50 min, respectively. The primary ions were set $[M + H]^+$ and $[M - H]^-$ in positive and negative mode respectively.

A target list was built based on common additives reported in the literature and ions detected in the plastic feedstocks but absent in the blank, selecting only the precursors. This list was then integrated into Metaboscape® 2024b, where the compounds were flagged, and the intensity of each ion was extracted and compared between the plastic charge and the effluent from the recycling process.

2.4.11. Thermal gradient interaction chromatography (TGIC). Thermal gradient interaction chromatography (TGIC) experiments were performed using a CEF/TGIC instrument from PolymerChar (Valencia, Spain). The instrument was equipped with a Hypercarb column from Thermo Scientific containing particles of graphitic carbon (average particle size 5 μm, pore size of 250 Å). The dimensions of the column were 100×4.6 mm^2 ($L \times$ ID). The samples at a concentration of 1 mg mL^{-1} were dissolved in 10 mL vials for 1 h at 150 °C with 1,2,4-trichlorobenzene (TCB) containing 300 ppm of butylated hydroxytoluene (BHT) and purged with nitrogen to protect the polymer against oxidative degradation. 200 μL of the sample solution was injected into the column at 160 °C. This technique requires a cooling (adsorption) and a heating (desorption) step. A cooling ramp of 20 °C min^{-1} to 40 °C was applied to promote polymer adsorption. Elution began isothermally at 40 °C for 5 min at a flow rate of 0.5 mL min^{-1}, followed by a heating ramp at 2 °C min^{-1} to desorb the polymer. An infrared detector was used to monitor the components' concentrations and compositions when the chains were eluted from the column.

The infrared detector (model IR5-MTC, PolymerChar, Valencia, Spain) is equipped with two cells. One sensor is sensitive to the stretching vibrations in the C–H bonds of methyl groups (CH$_3$ at 2960 cm^{-1}) and the second sensor is sensitive to the C–H bonds in the methylene groups (CH$_2$ at 2920 cm^{-1}). Since methyl groups indicate branches, it is possible to determine their number by using the IR detector directly. To quantify the methyl content in unknown samples for the calculation of the comonomer content, it is necessary to calibrate the IR detector with standards of known methyl content. We used ethylene–butene copolymers provided by PolymerChar and some of ethylene hexene copolymers synthesized in the laboratory as standards to calibrate the IR detector. For this calibration, the mol% of the comonomer was translated into a methyl number for 1000C (CH$_3$/1000C). In these conditions the methyl chain ends were neglected.

2.4.12. Size exclusion chromatography. A Polymer-Char GPC-IR (PolymerChar, Valencia, Spain) was used. Detection was performed with a filter-based multiple band IR detector (model IR5-MTC, PolymerChar, Valencia, Spain). As stationary phase, three PLgel Olexis analytical columns, 7.5×300 mm (PolymerChar, Valencia, Spain) were used. The MMD was evaluated using polystyrene calibration (EasiCal PS-1, Agilent, Waldbronn, Germany). The used software was WinGPC version 8 (PolymerChar, Valencia, Spain). The instrument was equipped with a 200 μL sample loop, which corresponds to the injection
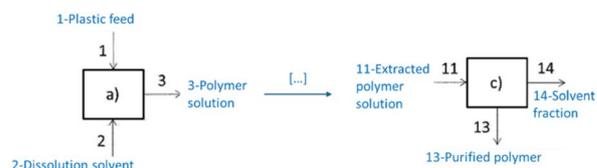

Fig. 1 Dissolution step (a) and recovery step (c), adapted from ref. 16.

volume. The mobile phase was 1,2,4 TCB, containing 0.4 g L^{-1} of BHT, and its flow rate was set at 1 mL min^{-1}. For each measurement, about 6 mg polymer was automatically dissolved in 8 mL of mobile phase. Simultaneously, the vials were flushed with nitrogen. Each sample was dissolved under shaking in the autosampler for 1 h at 150 °C before injection. The molar masses of PS standards were transferred to polyethylene equivalents using the following Mark–Houwink coefficients: KPP: $1.7 \times 10-4$ dL g^{-1}, [α]PP: 0.725 and KPS: $1.6 \times 10-4$ dL g^{-1}, [α]PS: 0.702.

2.4.13. Differential scanning calorimetry (DSC). Thermal analyses were performed using a METTLER TOLEDO DSC 3+ instrument under azote atmosphere. 40 μL aluminium hermetic pans were used to obtain the melting and crystallisation temperatures and the crystallinity. In all cases, a heating–cooling–heating cycle with an upper temperature of 200 °C and a heating rate of 10 °C was performed to remove the thermal history of the samples.

2.4.14. Dissolution vessel. In the recycling process, a dissolution and a recovery steps are involved.[16] A schematic representation is presented in Fig. 1.

We carried out dissolution and precipitation experiment at a lab scale in a glass reactor. The equipment consists of a 500 mL glass jacketed vessel, heated by an oil bath. The vessel was equipped with a cooled condenser to condense the evaporated solvent. The medium was mixed by a 4-blades propeller. The 12 mm diameter Raman probe, the 6 mm NIR probe and a temperature probe were inserted into the medium. An argon flow was put in the air of the vessel to avoid penetration of oxygen and polymer degradation during the dissolution. By this way, spectral changes were only due to polymer dissolution. For each experiment, the required amount of solvent was first introduced to the vessel. Then, the temperature was increased to the desired value using the heating bath. Once the temperature set point was reached, polypropylene was added (in "flakes" form or in powder form after cryogenic grinding of the pellets) at a known concentration.

After each experiment, the polymer solution was cooled down and precipitated using methanol at a ratio of solvent/antisolvent (S/AS) of 1 : 3. Then the precipitated polymer was washed again using methanol, filtrated and the residual solvent was evaporated by drying under vacuum at 110 °C and 104 Pa for 8 hours, followed by an additional drying at atmospheric pressure in an oven at 100 °C for 24–48 h.

2.5. Sampling, reference method and chemometrics

The sampling system, the gravimetry reference method as well as the calculation of error bars are based on a previous work.[17,18]

Different chemometric models are used to monitor the polymer concentration during the dissolution and precipitation steps.

Four different single-solvent partial least squares (PLS) models were built in xylene, decalin, TCB and n-decane. Twenty concentrations were accounted within a range of 0 to 20% and 20 temperatures within a range of 130 °C to 160 °C for each concentration, so 400 points per model.

Then a multi—solvent generalized model has been generated by combining the same data of all solvents and preprocessed using external parameter orthogonalization (EPO). The details of the models development are described in a previous work.[17,18]

3. Results and discussion

3.1. Plastic charge characterization

3.1.1. Polymer properties. Fig. 2 represent the characterization prior to recycling including the polymer properties and additives properties. Fig. 2(a) and (b) represent the DSC heating and cooling thermograms respectively, Fig. 2(c) represent the IR spectra of the plastics feedstocks and of a virgin PP, for comparison. Fig. 2(d) represent the HT-SEC molar mass distributions, Fig. 2(e) the TGIC profiles and finally Fig. 2(f) shows the LC-HRMS chromatogram (positive mode) of the different plastic feedstocks.

The melting and crystallization temperatures as well as the crystallinity are reported in Table S2. Furthermore, the presence of polymer contaminant in the main plastic feed stream has been detected. Indeed on Fig. 2(a), the heating (melting) curves reveal the presence of a second peak around 125 °C compared to the PP melting temperature which is around 164 °C. For the different plastic feedstocks, this suggests the presence of PE in PP. The same tendency has been observed on the crystallization curves (Fig. 2(b)). The structural properties are shown through the IR spectra Fig. 2(c), which shows the chemical nature of the polymer (i.e., PP) but more importantly the presence of additives. The polymers molar mass distributions are shown on Fig. 2(d). A similar molar mass distribution is recovered despite the different plastic charges analyzed. The presence of various polyolefins is reflected in the TGIC analysis. First, the peak at 119 °C corresponds to isotactic polypropylene (iPP), the main polymer in the plastic stream. A lower taticity PP peak is also present around 105 °C. Additionally, the residual HDPE contamination previously identified in DSC is also detected in TGIC at 137 °C. Also, a soluble fraction can also be observed (Fig. 2(e)) composed of amorphous PP (aPP) and amorphous PE (aPE).

3.1.2. Additives analysis. On Fig. 2(f), the LC-HRMS chromatogram of the different plastic feedstocks reveals a wide range of additives. This highlights the complexity and diversity of additives in the plastic feedstocks. The primary objective of these analyses is to assess additive removal efficiency by comparing samples before and after the dissolution/ precipitation cycle(s). As mentioned in the Method section, a target list has been compiled based on common additives previously annotated from literature and based on compounds detected in the charge and not present in the blank. A high number of additives were detected across all samples, both in positive and negative mode, highlighting the complexity of the waste streams.

A detailed non-target screening of the plastic feedstocks samples confirmed the presence of numerous substances across both positive and negative ionization modes, highlighting the compositional diversity of market-available plastics.

These were grouped into distinct families based on their retention times and structural similarities.

The identified families include glycerol-containing compounds, amines (such as dihydroxyalkyl amines and other aliphatic or aromatic amines), amides (including those with double bonds, bisamides, dihydroceramides, and other amide derivatives). Other classes were identified, including polyethylene glycols (PEGs), sulfonic compounds and other miscellaneous organics. Among them, a subset corresponded to typical functional and commercial additives such as light stabilizers, plasticizers, antioxidants, lubricants, clarifying agents and antistatic agents, reflecting the wide range of formulations used in commercial plastics.

These additives can pose challenges in the recycling process, either by affecting material properties or failing to meet evolving regulatory compliance. Therefore, it is crucial to precisely characterize their composition and assess their removal efficiency during recycling. All the additive's peak detected in LC-HRMS for the three plastic feedstocks were compiled in the target list. Subsequently, a comparative analysis of the additives before and after recycling is conducted to assess the effectiveness of additive removal. It can also be noted that the recompounding of wPP2 lead to a significant increase of the number of additives present in the polymer. This can question the efficiency of mechanical recycling, as it often relies on the addition of large amounts of additives to compensate for the degradation of polymer properties. This raises concerns about the long-term sustainability of mechanically recycled plastics and highlights the need for chemical and physical recycling methods, which aim to recover high-purity polymers while minimizing additive reliance.

3.2. Monitoring plastic charge dissolution

The second objective is to monitor in real time the dissolution and precipitation steps using in situ spectroscopy coupled to chemometrics.

3.2.1. In situ spectra analysis. Considering the wide range of additives that can be found in the plastic feedstocks (colorant, pigment, etc.), two main risks on the spectral signature of the polypropylene feedstocks are possible: the first one is the complete loss of signal due to fluorescence, fouling or medium coloration; the second one is that the additive response hides the polymer information thus requiring a deeper data treatment.

To resolve these doubts, a first look on the raw spectra is required. Only the Raman spectra are discussed here since discussing NIR spectra without chemometric treatment is irrelevant because of the complexity of the band attribution. Fig. S2
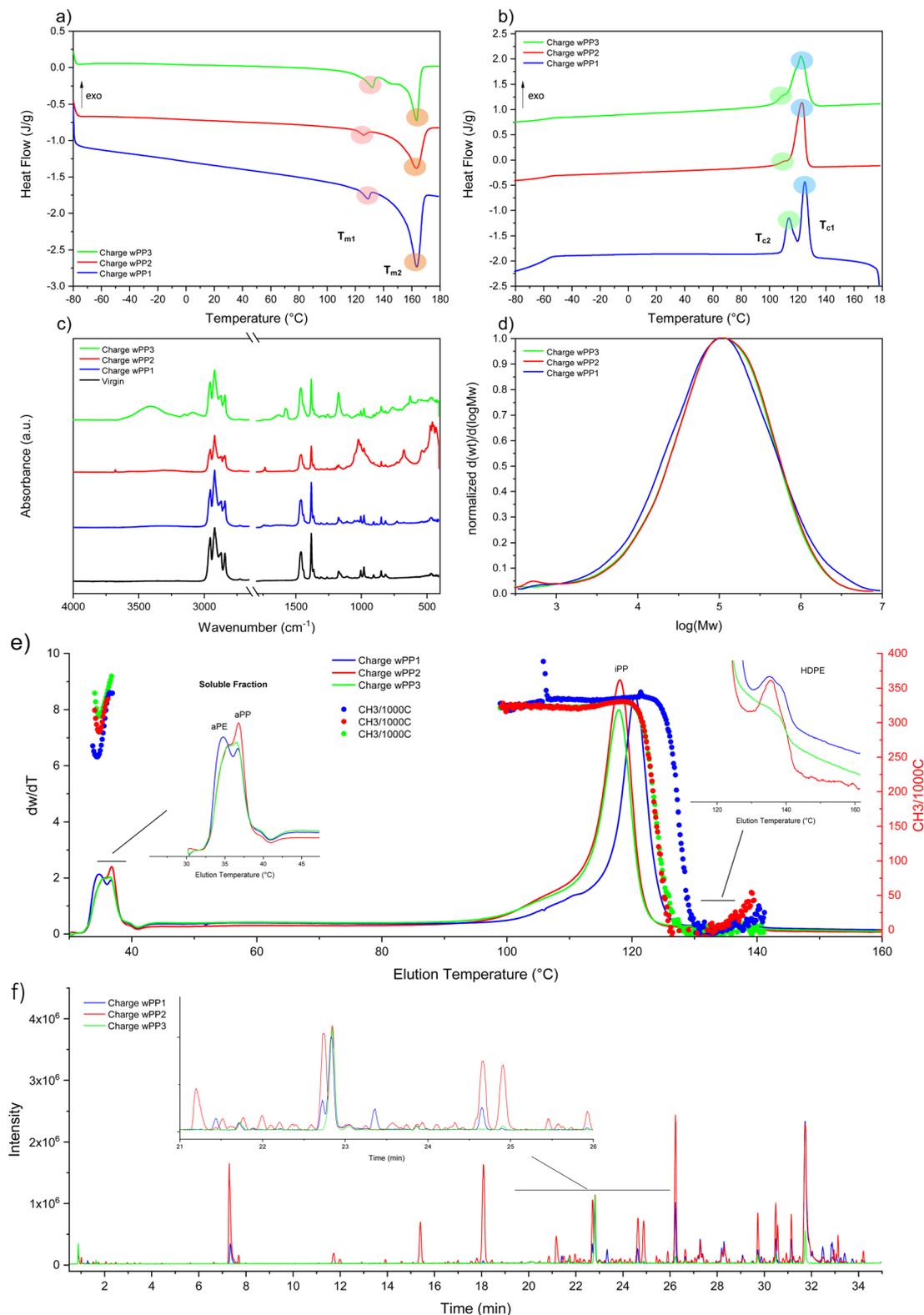
Fig. 2 (a) DSC heating (melting) curves and (b) DSC cooling (crystallization) curve of the different PP feedstocks where T_{m1} and T_{m2} represent the PE and PP melting temperatures, respectively and T_{c1} and T_{c2} represent the PE and PP crystallization temperatures respectively, (c) infrared spectra of the different PP feedstocks and a virgin PP (d) molar mass distributions of the different PP feedstocks (e) TGIC profiles of the different PP feedstocks where the 20–50 °C and 120–160 °C elution temperature windows were highlighted. The second axis represent the number of CH3/1000C (f) LC-HRMS chromatogram of the different PP feedstocks where the 21–26 min retention time window has been highlighted.

shows the raw Raman spectra of the solvent, pure PP/solvent, and PP charge/solvent systems once fully dissolved in xylene, decalin and *n*-decane. The spectra are clear, interpretable, and not impacted by the presence of contaminations.

Furthermore, in addition to the polypropylene bands, new bands which are not present either in the solvent or in the pure PP/solvent systems appear at 700 cm^{-1} and 1500 cm^{-1} (yellow overlining). This suggests a possible identification and quantification of additives during the recycling process using *in situ* Raman spectroscopy.

3.2.2. *In situ* spectroscopic monitoring. Different dissolution experiments were performed and monitored using NIR and Raman spectroscopy. We used the model developed on commercial polypropylene to predict the polymer content during the plastic feed dissolution.[17,25] The operating conditions are reported Table S3.

Fig. 3 shows the predictions by Raman spectroscopy for Runs 1, 2, and 3, where the plastic feed was introduced in the flakes form. The plot of the dissolved polypropylene content *versus* time shows a good prediction of the final value meaning that despite the presence of additives, the model (trained on commercial PP) can recover the polypropylene bands from the spectra of the plastic charge. However, a poor prediction of the dissolution dynamics is observed, particularly an overestimation of the polymer content. This is due to the form introduced. Indeed, in the flakes form, where the objects are quite big (order of cm) a fouling of the probe is observed during dissolution. When dissolving, the polymer flake swells and softens, so it become easier to stick on the probe which brings bias to the prediction by overestimating the polymer content. After a longer dissolution time, the polymer will decrystallize and disentangle, become more soluble and detach from the probe, so the prediction becomes accurate.

Run 1 and Run 3 are replicates and both prediction follows the same trend which confirms the hypothesis made.

To further demonstrate this hypothesis, the polymer raw material has been transformed into powder. The powder has been obtained by cryogenic grinding of the flakes which ensures that the polymer properties remain unchanged (molecular weight, branching, crystallinity, *etc.*) and only the form changes.

Runs 1, 2 and 3 from Table S3 were performed again whereas this time, the polymer form changed to powder (see Runs 4, 5 and 6). Fig. 3 shows the predictions of the new experiments. It can be seen that the final polymer content is well predicted as in the case of polymer flakes, but no overestimation of the concentration is observed. Note that the dissolution kinetic is faster due to the higher surface contact of the powder.

Fig. 4 shows the monitoring by NIR and Raman spectroscopy of the dissolution of the several polymer samples in powder form (wPP1, wPP2 and wPP3) in solvents used in the calibration set (*e.g.* decalin, run 7 Fig. 4(a)), mixtures of solvents (*e.g.* decane/decalin 50 : 50, run 8, Fig. 4(b)), and solvents not present in the calibration set (*e.g.* amyl acetate, run 9 as showed Fig. 4 c). A good prediction is obtained using NIR and Raman spectroscopy. Also, the dissolution rate in new solvents or mixtures of solvents was possible, due to the orthogonalization implemented during model development.[18]

3.3. Monitoring plastic charge precipitation

The dissolution-based recycling process usually includes several steps: (i) polymer dissolution, (ii) filtering to eliminate non-dissolved substances, (iii) optional washing with a dense solvent for the removal of the insoluble part, (iv) optional adsorption, and (v) recovery by precipitation. The final step of recovery of the polymer can either be performed by heating above the melting temperature of the polymer to evaporate the
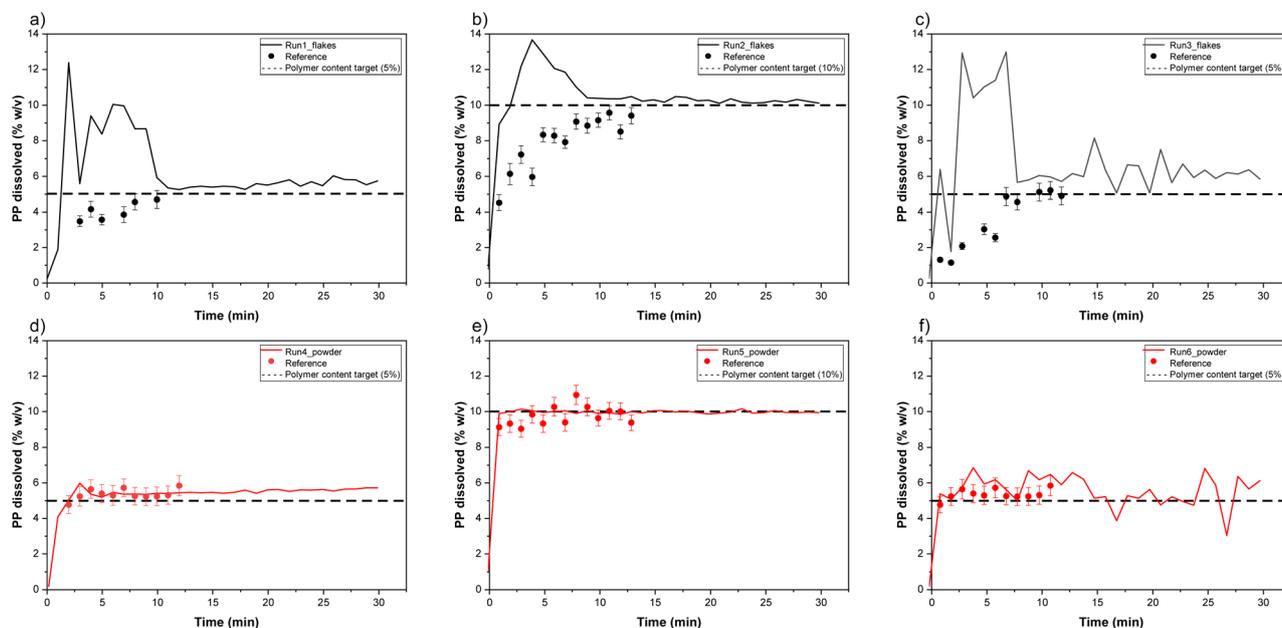

Fig. 3 Prediction of the polymer content by Raman spectroscopy and the reference method during (a) Run 1 (b) Run 2 (c) Run 3 (d) Run 4 (e) Run 5 and (f) Run 6.
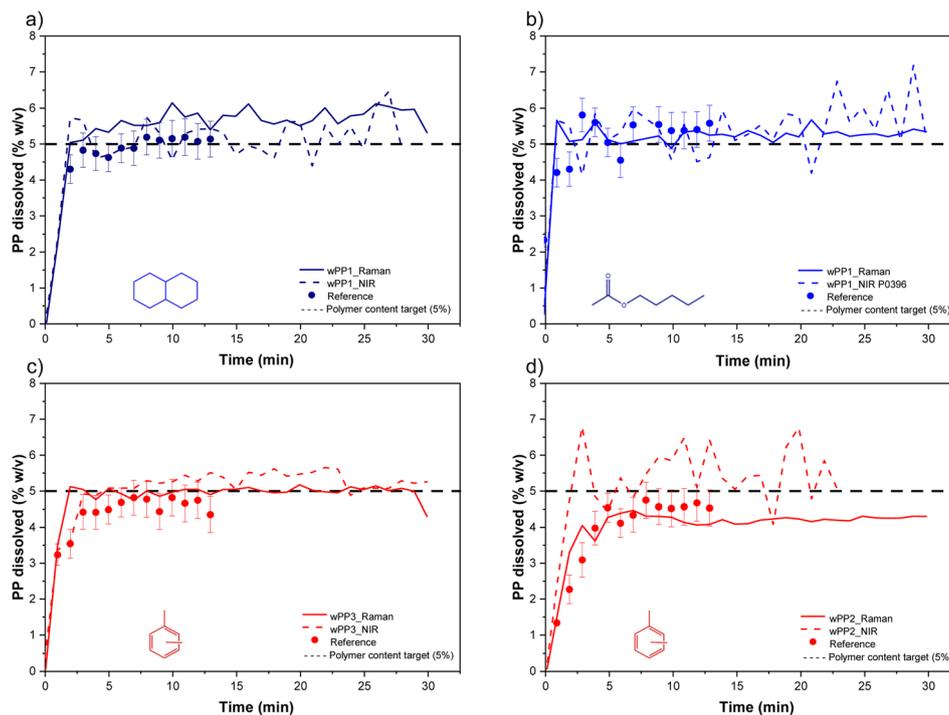
Fig. 4 Prediction of the polymer content in NIR and Raman during (a) Run 7, (b) Run 8 (c) Run 9 and (d) Run 10.

solvent, or by cooling to precipitate and recover a solid polymer. The second option has been chosen here due to the limitations of the available set-up, although it is not the best option for swelling reasons. Few works report the study of precipitation/crystallization of dissolved polymers and mainly involve concentrations below 0.5 wt%.[26,27]

We observed that with increasing the polymer content, a polymer "block" was formed during cooling, making stirring difficult so biasing *in situ* analysis. While it is non-productive to work at low concentrations, we investigated the maximum concentrations possible before reaching stirring issues. The interest of this is to determine the quality of the recovered polymer and to be able to evaluate its purification during recycling. Below 3 wt%, the polymer/solvent mixture precipitated under particle form during cooling. It is thus the concentration that has been chosen for the monitoring.

Fig. 5 shows the *in situ* monitoring during cooling of a pure PP compared to the wPP3 plastic charge stream by NIR and Raman spectroscopy.

As it can be observed by comparing the solution crystallization temperatures, the plastic charge PP has a lower crystallization temperature compared to pure PP. This is more clearly seen from the derivative curves. This suggests that the additives present in the plastic charge play the role of crystallization inhibitor due to their diversity.

Furthermore, to be able to qualify the polymer/additive's separation *in situ*, we need to compare this precipitation monitoring with the additives spectral signature. We have previously mentioned that we were able to detect an additive response on the *in situ* spectra (Section 3.2.1). Besides, performing a calibration with the identified compounds is

pointless in view of their large diversity. Instead, we proposed to use an unsupervised methodology to monitor the behavior of the additive during cooling of the dissolved plastic charge.

Fig. S3 shows the selected bands on the spectrum of the dissolved wPP3 plastic charge stream which correspond to the presence of other compounds besides the polymer by comparing with the spectra of pure solvent and pure PP/pure solvent system. It is thus expected that it represents a spectral response of the additives. Based on these selected wavelength regions, we performed a Principal Component Analysis (PCA) on the spectra during cooling of the plastic charge. The model quality was investigated to validate that the temperature effect was removed and that the monitoring was related to the additive behaviour. Fig. S4 shows that there is only 1 component explaining 99% of the variability which confirms that there is only one variability. The comparison of the polymer behaviour (PLS prediction) with the additive behaviour (PC1 scores) during cooling, is shown in Fig. 6.
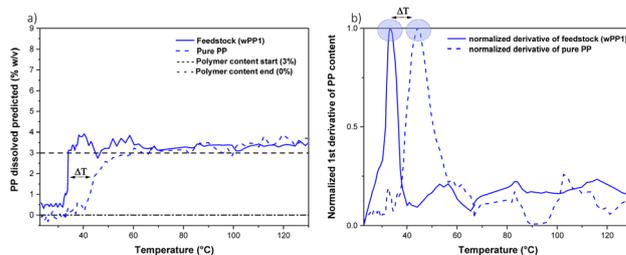

Fig. 5 (a) Prediction of the polymer content using NIR and Raman during cooling of run and (b) normalized 1st derivative of the corresponding spectroscopic signal.
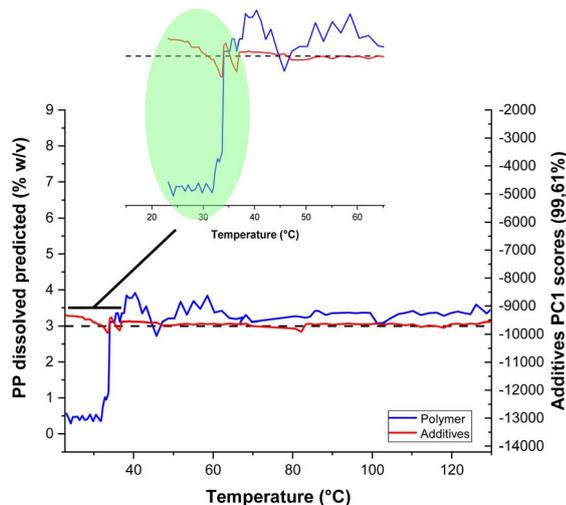
Fig. 6 Monitoring of both the supervised polymer content and unsupervised additive response (additives) and zoom on the lower temperatures.

The figure shows that while the predicted polymer content decreases (*i.e.*, the polymer precipitates), the additives spectral response remains constant (*i.e.*, the additives stay soluble). This indicated that the precipitation has been performed effectively and that we were able to monitor the separation of the additives from the polymer.

To confirm these observations, the recovered polymer has been characterized by LC-HRMS with the same protocol and with other analytical techniques to verify that it has kept its structure and properties.

As a reminder, after each experiment, the polymer was recovered by precipitating the solution with methanol (S/AS = 1 : 3), followed by filtration, methanol washing, and solvent removal through vacuum drying at 110 °C and atmospheric drying at 100 °C.

3.4. Recycled polymer characterization

The objective of this section is to investigate the impact of these operating conditions on the quality and properties of the

recovered recycled polymer, by combining *in situ* spectroscopic monitoring with complementary analytical techniques. For conciseness, the following section detail the tested operating conditions using abbreviations. The specific abbreviations associated with each condition are detailed in Table 1.

Fig. 7 shows the recovered polymer after one recycling compared to the original plastic charge, and the associated DSC thermograms and IR spectra for few experiments (DSC of the other experiments is given in Fig. S5). A slight discoloration can be observed for wPP2 and wPP3 whereas for wPP1 a dark grey powder has been obtained because of the mixing of several colours. The presence of the peak at 135 °C on the DSC heating thermograms was attributed to HDPE contamination and is still present after the recycling cycle. On the other hand, the IR spectra confirm that part of the additives has been removed as demonstrated by the lower intensities on their bands, around 750 cm^{-1} in the case of wPP2 and 3250 cm^{-1} for wPP3. The spectrum of the recycled polymer gets closer to that of the virgin polymer.

Fig. S5 shows the DSC thermograms and Fig. S6 the molar mass distributions for all the other operating conditions. Additionally, the associated data (recovery percentage, crystallinity, melting point and mass average molar mass) for each operating conditions has been reported Table 2.

The DSC analysis shows that the structure of the polymer remained the same with comparable melting point and crystallinity, except for the A1_2 condition of wPP1 and D2_1 condition of all plastic feedstocks which correspond to a longer dissolution time and higher dissolution temperature respectively. A double peak has also been observed on the DSC thermograms of recycled wPP3 in the D2_1 condition (Fig. S5) that suggest severe degradation.

The mass average molar mass (Table 2) and distributions (Fig. S6) remains the same prior and post recycling for the dissolution in amyl acetate, cyclohexanone and *n*-decane during 30 min at 130 °C. In the case of wPP1, when increasing the dissolution time from 30 min to 2 hours (A1_1 and A1_2 respectively), the mass average molar mass decreases by half. Indeed, when exposed to heat for a longer period, the polymer is more susceptible to degrade by chain-scission. In the same way, when increasing the temperature from 130 °C to 170 °C (D1_1

Table 1 Operating conditions of the plastic charge PP recycling

| Feed	Solvent	Temperature (°C)	Dissolution time (h)	Number of dissolution cycles	Abbreviation
wPP1	Amyl acetate	130	0.5	1st	A1_1
wPP1	Amyl acetate	130	2	1st	A1_2
wPP1	Cyclohexanone	130	0.5	1st	C1_1
wPP1	Decane	130	0.5	1st	D1_1
wPP1	Decane	170	0.5	1st	D1_2
wPP1	Decane	130	0.5	2nd	rD1_1
wPP2	Decane	130	0.5	1st	D1_1
wPP2	Decane	170	0.5	1st	D1_2
wPP2	Decane	130	0.5	2nd	rD1_1
wPP3	Decane	130	0.5	1st	D1_1
wPP3	Decane	170	0.5	1st	D1_2
wPP3	Decane	130	0.5	2nd	rD1_1
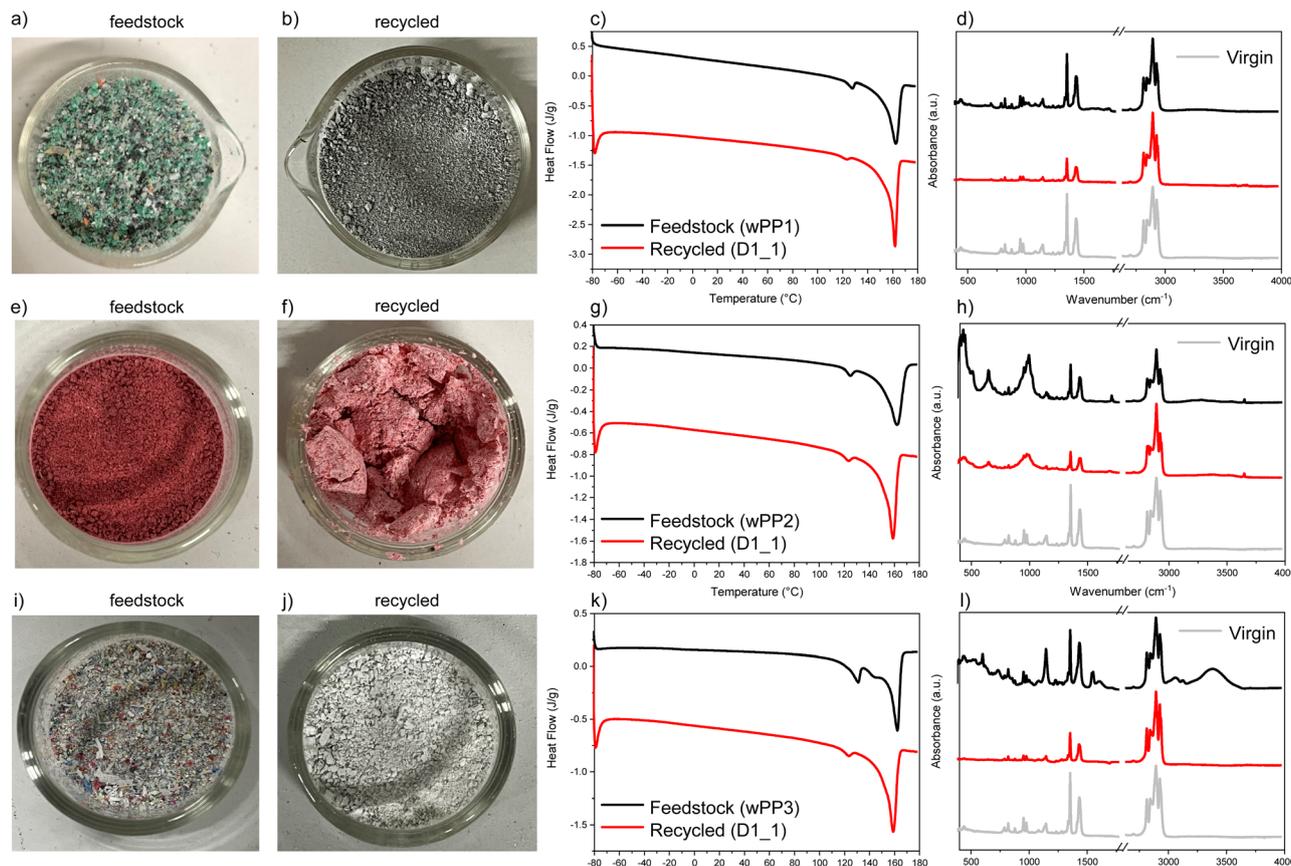
Fig. 7 (a) wPP1, (b) wPP1 recycled in *n*-decane at 130 °C during 30 min, (c) associated DSC heating thermograms, (d) associated IR spectra, (e) wPP2, (f) wPP2 recycled in decane at 130 °C during 30 min, (g) associated DSC heating thermograms, (h) associated IR spectra, (i) wPP3, (j) wPP3 recycled in *n*-decane at 130 °C during 30 min, (k) associated DSC heating thermograms, (l) associated IR spectra.

and D2_1 respectively), the mass average molar mass decreases from 256.6 kDa to 152.4 kDa for wPP1, from 250.2 kDa to 128.3 kDa for wPP2 and from 203.1 kDa to 38.1 kDa for wPP3. This indicated that wPP3 might have fewer protective additives against degradation (*e.g.* antioxidants).

A second recycling cycle has also been investigated (only for the D1_1 operating condition) where the recycled polymer is introduced again in the reactor and recycled the same way. Fig. S7 and S8 represent the DSC heating thermograms and the normalized molar mass distribution curves respectively.

The thermal and microstructural properties are highly impacted by the 2nd recycling cycle with lower melting points and decreased molar mass for wPP2 and wPP3. Interestingly, the properties of the recycled wPP1 are not impacted by a 2nd recycling cycle which might indicated that the additives responsible of protecting the polymer were not removed during the 1st cycle and still plays their role during the 2nd cycle. This hypothesis still must be verified by deeper analysis of the LC-HRMS chromatograms. At last, the operating conditions must be tuned in order to keep the polymer structure and properties while removing most of the additives. It's a compromise between a dissolution during 30 min that does not removes a lot of additives and one during 2 h that removes more additives but slightly degrade the polymer. The detail of all the HT-SEC

measurement is given Table S4. The second recycling cycle significantly impact the polymer properties as demonstrated by the TGIC profiles represented Fig. S9–S11 for the plastic charge wPP1, wPP2 and wPP3 and their effluents respectively. For the plastic charge wPP1, most conditions give similar TGIC profiles, meaning intact polymer properties. In the case of increasing dissolution time (Fig. S9, A1_1 and A1_2 condition), the iPP peak shifts from 121 °C to 118 °C and an increased in the peak of lower tacticity. This suggests that degradation may also induce changes in tacticity. Additionally, the increase in the soluble fraction with extended dissolution time further supports this observation. The increase in the soluble fraction can also be attributed to a degradation of the HDPE present because of the peak's decrease at 138 °C.

For the plastic charge wPP2 (Fig. S10), the second recycling cycle caused significant polymer degradation, as previously observed by HT-SEC. This degradation is further confirmed by TGIC, which shows a substantial increase in the soluble fractions, indicating a major change in tacticity.

No change was observed on Fig. S11 for the plastic charge wPP3 and the recycled material in the D1_1 condition. A step further would be to integrate *in situ* monitoring of the degradation.[28]

Table 2 Thermal and structural properties of the plastic charge polymer materials before and after recycling

Sample	Operating conditions	Recovery (%)	T_m (°C)			Crystallinity (%)			M_w (kg mol^{-1})		
			Feed	Recycled	2nd cycle	Feed	Recycled	2nd cycle	Feed	Recycled	2nd cycle
wPP1	A1_1[a]	98.6	164.3	163.2	—	34.9	35.7	—	248.1	255.8	—
	A1_2[b]	93.6		159.8	—		36.4	—		108.8	—
	C1_1[c]	92.3		163.5	—		36.6	—		258.8	—
	D1_1[d]	93.1		163.7	164.2		38.4	34.9		256.6	241.2
	D2_1[e]	92.6		160.8	—		38.2	—		152.4	—
wPP2	D1_1	94.3	164.1	160.7	151.2[f]	27.5	23.0	18.3	249.3	250.2	11.4
	D2_1	94.0		159.6	—		24.6	—		128.3	—
wPP3	D1_1	99.5	164.2	161.1	150.7[f]	27.5	31.6	38.3	249.4	203.1	9.9
	D2_1	92.5		156.4[f]	—		29.4	—		38.1	—

[a] Amyl acetate, 130 °C, 30 min. [b] Amyl acetate, 130 °C, 120 min. [c] Cyclohexanone, 130 °C, 30 min. [d] n-Decane, 130 °C, 30 min. [e] n-Decane, 170 °C, 30 min. [f] Double peak observed on the heating thermogram.

Finally, LC-HRMS informs us on the additive's removal quality (Fig. 8). The chromatograms of both the plastic feed wPP2 and recycled polymer in the D1_1 condition are shown. As we can observe, after recycling, most of the additive's peaks are removed, or decreased in intensity. Nevertheless, there are still some peaks that remain, indicating that one recycling cycle has not been 100% efficient.

To further interpret these results, one representative additive from each major family was monitored before and after recycling in the D1_1 condition. This targeted approach allowed us to identify which families are more resistant to removal, revealing, for instance, that certain high-molecular-weight antioxidants and lubricants remain partially retained within the polymer, whereas lighter or more polar additives are more efficiently extracted.

For instance, Irganox 245 (RT = 24.2 min; $[M + H]^+$, m/z = 587.3578; $[M + NH_4]^+$, m/z = 604.3850; $[M + Na]^+$, m/z = 609.3396; $C_{34}H_{50}O_8$) was selected as a representative antioxidant, Tinuvin 770 (RT = 7.6 min; $[M + 2H]^{2+}$, m/z = 241.2040; $[M + H]^+$, m/z = 481.4003; $C_{28}H_{52}N_2O_4$) represented the light stabilizer family. Citroflex A-4 (RT = 22.3 min; $[M + H]^+$, m/z = 403.2326; $[M + Na]^+$, m/z = 425.2143; $C_{20}H_{34}O_8$) was chosen as a plasticizer, and oleamide (RT = 23.3 min; $[M + H]^+$, m/z = 282.2793; $[2M + H]^+$, m/z = 563.5512; $[2M + Na]^+$, m/z = 585.5335; $C_{18}H_{35}NO$) as a model amide compound. Additionally, Erucamide (RT = 26.5 min; $[M + H]^+$, m/z = 338.3419; $[M + Na]^+$, m/z = 360.3231; $[2M + H]^+$, m/z = 675.6760; $C_{22}H_{43}NO$) was monitored as a lubricant, and PEG Laureth-3 (RT = 21.1 min; $[M + H]^+$, m/z = 319.2843; $[M + Na]^+$, m/z = 341.2664; $C_{18}H_{38}O_4$) as a surfactant.

Note that the reported compounds are proposed annotations based on accurate mass measurements and comparison with literature data.[29–33] A deeper structural analysis, supported by standards or complementary analytical techniques, would be required to fully confirm the molecular structures.

These selected molecules serve as markers to evaluate additive removal efficiency across different chemical families. Comparing their chromatographic profiles before and after recycling allows identifying which classes of additives are more resistant to extraction and tend to remain within the polymer matrix, providing valuable insight into the mechanisms governing additive retention or release during solvent-based recycling.

Lighter and more polar additives were efficiently extracted during the dissolution step, with a clear decrease in their chromatographic signals after recycling, specifically majority of
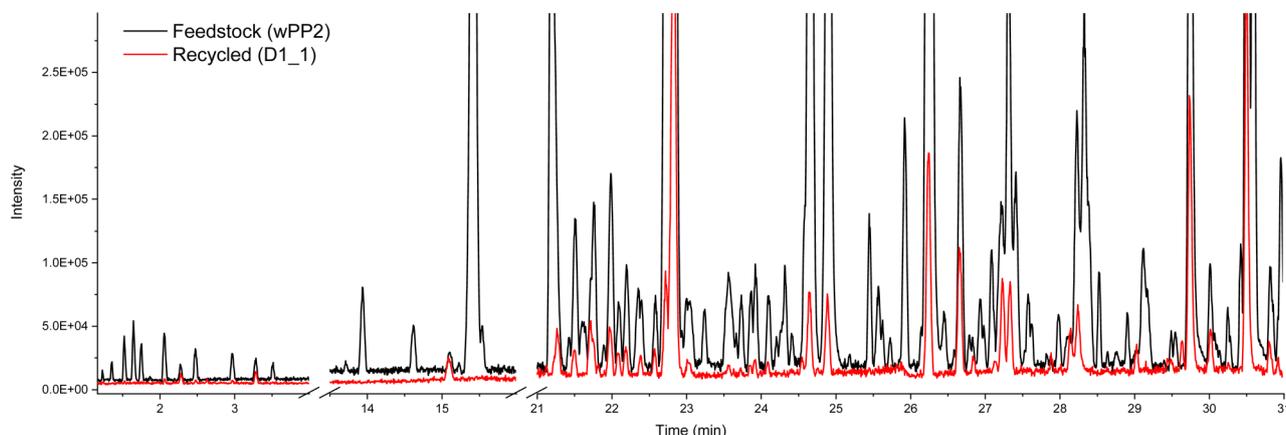

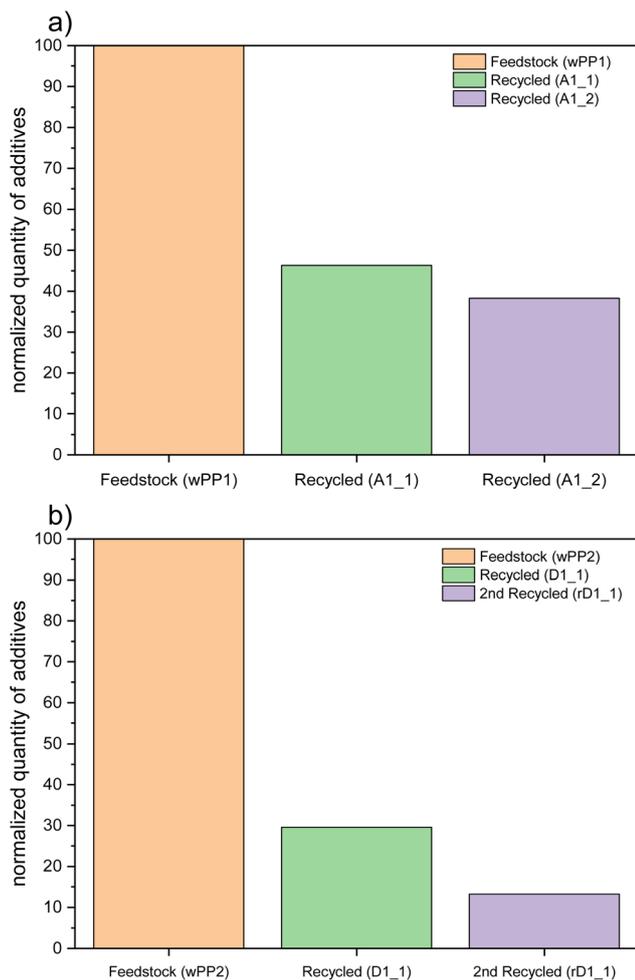**Fig. 8** LC-HRMS chromatogram of the plastic charge wPP2 and the recycled polymer in the D1_1 operating condition.

Fig. 9 Normalized quantity of additives obtained from the semi-quantitative approach for wPP1 and the recycled polymer during A1_1 and A1_2 operating condition (a) and for wPP2 and the recycled polymer during D1_1 and rD1_1 operating condition (b).

peaks until 21 minutes of elution. High-molecular-weight antioxidants and long-chain lubricants were more persistent, suggesting stronger interactions with the polymer matrix or limited diffusion out of the swollen polymer domains (around 30 min of elution). The other compounds showed intermediate behavior, with partial removal depending on molecular polarity and affinity with the solvent system.

The persistence of certain additives indicates that optimizing solvent selection and operating conditions could further improve purification. A more exhaustive structural identification, quantification, and correlation with polymer–additive interactions will be the subject of future studies aimed at refining solvent-based purification strategies and understanding additive retention mechanisms in complex waste streams.

Fig. 9 shows the comparison of the quantity of additives detected in LC-HRMS prior and post-recycling.

Under the A1_1 condition, approximately 60% of the additives were removed. Extending the dissolution time from 30 minutes to 2 hours (A1_2) resulted in only an additional 8%

removal, suggesting that dissolution time may not be the most critical parameter for additive elimination and that a shorter duration is sufficient. Furthermore, as shown in Table 1, a significant decrease in molar mass is observed between these conditions, dropping from 256 kg mol^{-1} to 109 kg mol^{-1}.

More conditions must be explored to better understand the role of additives in the recycling process and determine the optimal recycling parameters. Additionally, additive identification is a key aspect of this work, monitoring the presence of additives, ensuring regulatory compliance, and assessing their impact on material performance.

4. Conclusions

This work focuses on the development of analytical tools to control and understand the dissolution-based recycling process of polypropylene. A prior recycling characterization revealed that polymer contamination (HDPE in PP) could appear and that a simple dissolution/precipitation cycle is not enough to remove this contamination possibly impacting the mechanical properties. Also, LC-HRMS has been used to compare the additives prior and post-recycling, making this technique highly promising for deeper insights into the recycling process and its impact on material composition. We also performed prediction of plastic feedstock polypropylene content during dissolution and precipitation using NIR and Raman predictive models that were previously developed using commercial pure polypropylene in different solvents and at different temperatures. Despite the presence of additives in the plastic feedstocks (colorant, pigments, etc.), the outcomes of this method reveal the possibility of monitoring plastic feedstock polypropylene dissolution. Furthermore, the results highlight the importance of the form/size of polymer particles. The effect of particle morphology was also identified: while large flakes led to probe fouling and deviations in the predicted concentrations, reshaping the polymer into a powder ensured stable monitoring. With this adjustment, the methodology was successfully applied across several solvents, including mixtures and external solvents not present in the calibration set. The performances of the NIR and Raman predictions are comparable. Additionally, the precipitation step could be monitored and a different behavior between the polymer (which precipitates) and the additives (which remain dissolved) have been observed suggesting that we can evaluate the quality of the recycling process during the precipitation step in real time.

This study opens the doors to the implementation of process analytical technology (PAT) tools and specifically spectroscopy to polymer recycling pilots for its supervision. The present work has been applied to the monitoring of different plastic feedstock streams representative of sorting centres. But other plastic feedstock streams could be targeted like mixed plastic feedstock streams with more or less polypropylene content in the stream to see if the model is robust enough to predict accurately the polymer content or if it needs to be improved.

Based on these results, which demonstrated the potential of combining analytical techniques such as NIR, Raman, LC-HRMS, and TGIC to monitor and understand the dissolution-

based recycling process of PP, the importance of real-time process supervision and pre-recycling characterization to ensure material quality and performance were highlighted. Notably, the persistence of PE contamination in the recycled PP stream and the influence of additives and particle morphology emphasized that a simple dissolution/precipitation cycle may be insufficient for full purification.

Author contributions

Conflicts of interest

The authors declare no conflict of interest.

Data availability

All data generated or analyzed during this study are included in this article and its supplementary information (SI). Supplementary information: detailed synthetic methodologies and additional experimental results, including all the DSC thermograms, HT-SEC molar mass distributions, pictures of the plastic feedstock, and TGIC profiles. See DOI: https://doi.org/10.1039/d5su00571j.

Acknowledgements

References

1 R. Kol, R. Denolf, G. Bernaert, D. Manhaeghe, E. Bar-Ziv, G. W. Huber, N. Niessner, M. Verswyvel, A. Lemonidou, D. S. Achilias and S. De Meester, *ACS Sustainable Chem. Eng.*, 2024, **12**, 4619–4630.
2 I. Georgiopoulou, G. D. Pappa, S. N. Vouyiouka and K. Magoulas, *Resour., Conserv. Recycl.*, 2021, **165**, 105268.
3 M. Ramírez-Martínez, S. L. Aristizábal, G. Szekely and S. P. Nunes, *Green Chem.*, 2023, **25**, 966–977.
4 S. C. Aparício, P. M. Castro, B. D. Ribeiro and I. M. Marrucho, *Green Chem.*, 2024, **26**, 6799–6811.
5 S. Peng, S. Liang and M. Yu, *Procedia Environ. Sci.*, 2012, **16**, 327–334.
6 T. W. Walker, N. Frelka, Z. Shen, A. K. Chew, J. Banick, S. Grey, M. S. Kim, J. A. Dumesic, R. C. Van Lehn and G. W. Huber, *Sci. Adv.*, 2020, **6**, eaba7599.
7 K. Kaiser, M. Schmid and M. Schlummer, *Recycling*, 2018, **3**, 1.
8 K. L. Sánchez-Rivera, P. Zhou, M. S. Kim, L. D. González Chávez, S. Grey, K. Nelson, S.-C. Wang, I. Hermans, V. M. Zavala, R. C. Van Lehn and G. W. Huber, *ChemSusChem*, 2021, **14**, 4317–4329.
9 J. Yu, A. del C. Munguía-López, V. S. Cecon, K. L. Sánchez-Rivera, K. Nelson, J. Wu, S. Kolapkar, V. M. Zavala, G. W. Curtzwiler, K. L. Vorst, E. Bar-Ziv and G. W. Huber, *Green Chem.*, 2023, **25**, 4723–4734.
10 A. M. Lines, G. B. Hall, S. Asmussen, J. Allred, S. Sinkov, F. Heller, N. Gallagher, G. J. Lumetta and S. A. Bryan, *ACS Sens.*, 2020, **5**, 2467–2475.
11 R. A. M. Vieira, C. Sayer, E. L. Lima and J. C. Pinto, *J. Appl. Polym. Sci.*, 2002, **84**, 2670–2682.
12 M. M. Reis, P. H. H. Araújo, C. Sayer and R. Giudici, *Ind. Eng. Chem. Res.*, 2004, **43**, 7243–7250.
13 D. Fischer, K. Sahre, M. Abdelrhim, B. Voit, V. B. Sadhu, J. Pionteck, H. Komber and J. Hutschenreuter, *C. R. Chim.*, 2006, **9**, 1419–1424.
14 E. Hirsch, H. Pataki, J. Domján, A. Farkas, P. Vass, C. Fehér, Z. Barta, Z. K. Nagy, G. J. Marosi and I. Csontos, *Biotechnol. Prog.*, 2019, **35**, e2848.
15 T. De Beer, A. Burggraeve, M. Fonteyne, L. Saerens, J. P. Remon and C. Vervaet, *Int. J. Pharm.*, 2011, **417**, 32–47.
16 W. Weiss, D. L. Le Cocq, M. Sibeaud and A. H. Ahmadi-Motlagh, *WO pat.*, 2022128490A1, 2022.
17 S. Ferchichi, N. Sheibat-Othman, O. Boyron, C. Bonnin, S. Norsic, M. Rey-Bayle and V. Monteil, *Anal. Methods*, 2024, **16**, 3109–3117.
18 S. Ferchichi, N. Sheibat-Othman, M. Rey-Bayle and V. Monteil, *Anal. Chim. Acta*, 2025, **1380**, 344752.
19 Z. Liu, H. Yu, L. Lu, X. Lv, G. Ju, J. Zhao, F. Sun, Y. Wang and W. Yu, *J. Food Prot.*, 2023, **86**, 100121.
20 M. J. Martínez-Bueno, M. J. Gómez Ramos, A. Bauer and A. R. Fernández-Alba, *TrAC, Trends Anal. Chem.*, 2019, **110**, 191–203.
21 H. Mohammed Taha, R. Aalizadeh, N. Alygizakis, J. P. Antignac, H. P. H. Arp, R. Bade, N. Baker, L. Belova, L. Bijlsma, E. E. Bolton, W. Brack, A. Celma, W. L. Chen, T. Cheng, P. Chirsir, Ľ. Čirka, L. A. D'Agostino, Y. Djoumbou Feunang, V. Dulio, S. Fischer, P. Gago-Ferrero, A. Galani, B. Geueke, N. Głowacka, J. Glüge, K. Groh, S. Grosse, P. Haglund, P. J. Hakkinen, S. E. Hale, F. Hernandez, E. M. L. Janssen, T. Jonkers, K. Kiefer, M. Kirchner, J. Koschorreck, M. Krauss, J. Krier, M. H. Lamoree, M. Letzel, T. Letzel, Q. Li, J. Little, Y. Liu, D. M. Lunderberg, J. W. Martin, A. D. McEachran, J. A. McLean, C. Meier, J. Meijer, F. Menger, C. Merino, J. Muncke, M. Muschket, M. Neumann, V. Neveu, K. Ng, H. Oberacher, J. O'Brien, P. Oswald, M. Oswaldova, J. A. Picache, C. Postigo, N. Ramirez, T. Reemtsma,

J. Renaud, P. Rostkowski, H. Rüdel, R. M. Salek, S. Samanipour, M. Scheringer, I. Schliebner, W. Schulz, T. Schulze, M. Sengl, B. A. Shoemaker, K. Sims, H. Singer, R. R. Singh, M. Sumarah, P. A. Thiessen, K. V. Thomas, S. Torres, X. Trier, A. P. van Wezel, R. C. H. Vermeulen, J. J. Vlaanderen, P. C. von der Ohe, Z. Wang, A. J. Williams, E. L. Willighagen, D. S. Wishart, J. Zhang, N. S. Thomaidis, J. Hollender, J. Slobodnik and E. L. Schymanski, *Environ. Sci. Eur.*, 2022, **34**, 1–26.

22 H. Wiesinger, Z. Wang and S. Hellweg, *Environ. Sci. Technol.*, 2021, **55**, 9339–9351.

23 C. M. Hansen, *Hansen Solubility Parameters: A User's Handbook, Second Edition*, CRC Press, Boca Raton, 2nd edn, 2007.

24 A. A. Cuthbertson, C. Lincoln, J. Miscall, L. M. Stanley, A. K. Maurya, A. S. Asundi, C. J. Tassone, N. A. Rorrer and G. T. Beckham, *Green Chem.*, 2024, **26**, 7067–7090.

25 S. Ferchichi, F. Collas, O. Boyron, M. Rey-Bayle, V. Monteil and N. Sheibat-Othman, *Macromol. Chem. Phys.*, 2025, e00088.

26 A. J. Pennings, *J. Polym. Sci., Part C, Polym. Symp.*, 1967, **16**, 1799–1812.

27 S. Cheruthazhekatt, D. D. Robertson, M. Brand, A. van Reenen and H. Pasch, *Anal. Chem.*, 2013, **85**, 7019–7023.

28 S. Ferchichi, N. Sheibat-Othman, O. Boyron, S. Norsic, M. Rey-Bayle and V. Monteil, *Macromol. Rapid Commun.*, 2025, **46**, 2400748.

29 Q.-Z. Su, P. Vera and C. Nerín, *Anal. Chem.*, 2023, **95**, 8780–8788.

30 P. Vera, E. Canellas and C. Nerín, *Talanta*, 2018, **188**, 750–762.

31 Y. Sapozhnikova, *Talanta*, 2021, **226**, 122120.

32 Y. Sapozhnikova, A. Nuñez and J. Johnston, *J. Chromatogr. A*, 2021, **1651**, 462261.

33 J. Park, H. Yun, C. Yoon, K. Lee and K.-D. Zoh, *Environ. Eng. Res.*, 2023, **29**, 230123.